Theoretical study of h-abstraction reactions from CH 3Cl and CH 3Br Molecules by ClO and BrO Radicals

ARTICLE *in* THE JOURNAL OF PHYSICAL CHEMISTRY A · APRIL 2012

Impact Factor: 2.69 · DOI: 10.1021/jp301557c · Source: PubMed

5 AUTHORS, INCLUDING:

Sebastien Canneaux
Université des Sciences et Technologies de Lill…
31 PUBLICATIONS **248** CITATIONS
SEE PROFILE

Hammaecher Catherine
Université des Sciences et Technologies de Lill…
11 PUBLICATIONS **33** CITATIONS
SEE PROFILE

Florent Louis
Université des Sciences et Technologies de Lill…
45 PUBLICATIONS **401** CITATIONS
SEE PROFILE

Marc Ribaucour
Université des Sciences et Technologies de Lill…
36 PUBLICATIONS **1,022** CITATIONS
SEE PROFILE

THE JOURNAL OF PHYSICAL CHEMISTRY A

Article

pubs.acs.org/JPCA

Theoretical Study of H-Abstraction Reactions from CH_3Cl and CH_3Br Molecules by ClO and BrO Radicals

Sébastien Canneaux,*[,†] Catherine Hammaecher,[‡] Thibaud Cours,[§] Florent Louis,[†] and Marc Ribaucour[†]

[†]PhysicoChimie des Processus de Combustion et de l'Atmosphère (PC2A), UMR CNRS 8522, Bât. C11 and [‡]Université Lille1 Sciences et Technologies, Cité scientifique, 59655 Villeneuve d'Ascq Cedex, France

[§]Groupe de Spectrométrie Moléculaire et Atmosphérique (GSMA), UMR CNRS 7331, Faculté des Sciences, Université de Reims Champagne-Ardenne, BP 1039, 51687 Reims Cedex 2, France

Supporting Information

ABSTRACT: The rate constants of the H-abstraction reactions from CH_3Cl and CH_3Br molecules by ClO and BrO radicals have been estimated over the temperature range of 300−2500 K using four different levels of theory. Calculations of optimized geometrical parameters and vibrational frequencies are performed using B3LYP and MP2 methods combined with the cc-pVTZ basis set. Single-point energy calculations have been carried out with the highly correlated ab initio coupled cluster method in the space of single, double, and triple (perturbatively) electron excitations CCSD(T) using the cc-pVTZ and cc-pVQZ basis sets. Canonical transition-state theory combined with an Eckart tunneling correction has been used to predict the rate constants as a function of temperature. In order to choose the appropriate levels of theory with chlorine- and bromine-containing species, the reference reaction Cl ($^2P_{3/2}$) + CH_3Cl → HCl + CH_2Cl (R_{ref}) was first theoretically studied because its kinetic parameters are well-established from numerous experiments, evaluation data, and theoretical studies. The kinetic parameters of the reaction R_{ref} have been determined accurately using the CCSD(T)/cc-pVQZ//MP2/cc-pVTZ level of theory. This level of theory has been used for the rate constant estimation of the reactions ClO + CH_3Cl (R_1), ClO + CH_3Br (R_2), BrO + CH_3Cl (R_3), and BrO + CH_3Br (R_4). Six-parameter Arrhenius expressions have been obtained by fitting to the computed rate constants of these four reactions (including cis and trans pathways) over the temperature range of 300−2500 K.

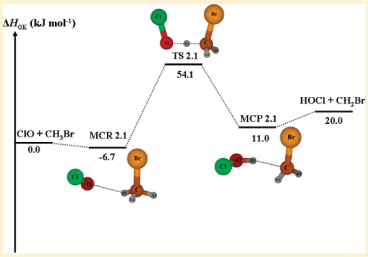

1. INTRODUCTION

The combustion model for thermal degradation processes of halogenated compounds in methane flames requires knowledge of thermodynamic and kinetic data. One of the most difficult problems from the experimental point of view is the determination of the temperature dependence of the kinetics of reactions over a wide temperature range. Most experimental measurements just provide overall rate constants and do not give details about the temperature dependence of the mechanism and the kinetics of individual pathways involved in the reactions. For many chlorinated and brominated species, there is little or no information about the kinetics and the mechanism of elementary reactions at high temperature. It is particularly the case for the XO + CH_3X molecular systems (X = Cl, Br).

Urey and Johnston[1] observed diffuse emission bands attributed to ClO radicals from a H_2−O_2 flame doped with Cl_2. The same flame was later studied by Pannetier and Gaydon,[2] and the positions of 19 bands were measured. A study[3] of the ignition and combustion of ammonium perchlorate in a hydrogen atmosphere showed that ClO radicals are generated at 1400 K near the surface of the burner at the same level of concentration as the OH radicals. It was the first time that the ClO radicals have been experimentally detected in flames including chlorinated compounds. Studies[4] of the equilibrium product distributions associated with the combustion of CH_3Cl, CH_2Cl_2, and $CHCl_3$ in air show that the mole fractions of ClO radicals under fuel lean conditions (equivalence ratio $\varphi = 0.5$) are at least 100 higher than those of OH radicals at temperatures lower than 900 K. As part of their work on the effect of chlorine on the oxidation of hydrocarbons, a two-parameter Arrhenius expression has been proposed by Ho et al.[5] for the reaction of the ClO radical with CH_3Cl. These kinetic parameters were estimated from the best available thermochemical data in 1992. The reported expression was the following: k (in cm^3 molecule^{-1} s^{-1}) = 5.0×10^{-13} exp(−44.8 (kJ mol^{-1})/RT)). This expression has been implemented in a chemical kinetic mechanism used to model the chemistry for chlorinated species in methane flames.

The electronic spectrum of the A $^2\Pi_i$ ← X $^2\Pi_i$ system of BrO was first observed by Vaidya.[6] Only a few band positions were measured, and an incomplete vibrational analysis was undertaken. The emission spectrum was also observed when bromine or CH_3Br was added to an oxygen−hydrogen flame.[7] There is no rate constant reported in the literature for the reactions of CH_3Br with bromine oxide radical BrO.

Received: February 16, 2012
Revised: March 20, 2012
Published: April 24, 2012

Table 1. Literature Kinetic Parameters for the Reaction Cl ($^2P_{3/2}$) + CH_3Cl → HCl + CH_2Cl (R_{ref})

A, cm^3 molecule^{-1} s^{-1}	E_a, kJ mol^{-1}	k, cm^3 molecule^{-1} s^{-1}	T, K	method	reference
2.17×10^{-11}	9.39		200−300	evaluation	Sander et al.[9]
		4.9×10^{-13}	298		
2.8×10^{-11}	9.98		222−298	evaluation	Orlando[10]
		4.99×10^{-13}	298		
3.3×10^{-11}	10.39		233−322	evaluation	Atkinson et al.[11]
		5.12×10^{-13}	300		
7.56×10^{-12} $(T/298\ K)^{0.92}$	6.61		300−843	DF/RF[a]	Bryukov et al.[12]
		5.37×10^{-13}	300		
		4.78×10^{-13}	295	P/FTIR[b]	Wallington et al.[13]
2.94×10^{-11}	10.06		281−368	P/GC[c]	Tschuikow-Roux et al.[14]
		5.21×10^{-13}	300		
3.35×10^{-11}	10.39		233−322	FP/RF[d]	Manning and Kurylo[15]
		5.2×10^{-13}	300		
2.13×10^{-10}	14.88		300−604	EB/MS[e]	Clyne and Walker[16]
		5.45×10^{-13}	300		
5.65×10^{-11}	13.80		271−598	DP/GC[c]	Knox[17]
		2.23×10^{-13}	300		
5.25×10^{-11}	12.89		357−477	DP/GC[c]	Goldfinger et al.[18]
		1.09×10^{-12}	400		
9.47×10^{-11}	14.05		298−484	P[f]	Pritchard et al.[19]
		3.39×10^{-13}	300		
3.71×10^{-11}	11.22		300−400	theory[g]	Senkan and Quam[20]
		4.11×10^{-13}	300		
		0.6×10^{-13}	298	theory[h]	Rayez et al.[21]

[a]DF/RF: discharge flow/resonance fluorescence. [b]P/FTIR: photolysis/Fourier transform infrared spectroscopy. [c]P/GC: photolysis/gas chromatography. [d]FP/RF: flash photolysis/resonance fluorescence. [e]EB/MS: electron beam/mass spectrometry. [f]P: photolysis. [g]Based on structure−activity relationship calculations and transition-state theory. [h]BAC-MP4 calculations and transition-state theory.

To assess the relevance of the title reactions in combustion conditions, it is important to understand their mechanism and their kinetics. In this work, the rate constants of the reactions ClO + CH_3Cl and BrO + CH_3Br will be estimated using the combination of quantum chemistry tools, statistical thermodynamics, and the transition state theory (TST). This theoretical study has been also extended to the halogen cross reactions ClO + CH_3Br and BrO + CH_3Cl, for which there are no kinetic data available in the literature. From the theoretical point of view, one of the most difficult problems is the accurate determination of the rate constants. The vibrationally adiabatic barrier therefore has to be determined with a great accuracy. In our previous work concerning the reactivity of iodine compounds,[8] it has been shown that the estimated rate constants strongly depend on the level of theory. At least 19 levels of theory were used to estimate the rate constants, which were compared to the available literature values over the temperature range of 250−2500 K. This methodological work[8] allowed demonstration that some of these levels of theory are adequate to obtain quantitative rate constants for the reactions involving iodine-containing species. Among them, the level of theory CCSD(T)/cc-pVQZ//MP2/cc-pVTZ provides a very good agreement between literature and calculated data for the studied reactions.

In order to choose the appropriate levels of theory with chlorine- and bromine-containing species, the reference reaction

$$Cl\ (^2P_{3/2}) + CH_3Cl \rightarrow HCl + CH_2Cl \qquad (Rref)$$

was first theoretically studied because the kinetic parameters have been well-established from numerous experiments, evaluation data, and theoretical studies since the 1950s.[9−21] The corresponding values are given in Table 1. The recommended value of the rate constant at 298 K by Sander et al.[9] is 4.9×10^{-13} cm^3 molecule^{-1} s^{-1}.

The H-abstraction reaction from a CH_3X molecule by a XO radical (X = Cl, Br) can a priori proceed by two pathways on the potential energy surface (PES), either the cis or the trans pathway. The following reactions are therefore studied:

$$ClO + CH_3Cl \rightarrow HOCl + CH_2Cl \qquad \text{cis pathway} \qquad (R1.1)$$

$$ClO + CH_3Cl \rightarrow HOCl + CH_2Cl \qquad \text{trans pathway} \qquad (R1.2)$$

$$ClO + CH_3Br \rightarrow HOCl + CH_2Br \qquad \text{cis pathway} \qquad (R2.1)$$

$$ClO + CH_3Br \rightarrow HOCl + CH_2Br \qquad \text{trans pathway} \qquad (R2.2)$$

$$BrO + CH_3Cl \rightarrow HOBr + CH_2Cl \qquad \text{cis pathway} \qquad (R3.1)$$

$$BrO + CH_3Cl \rightarrow HOBr + CH_2Cl \qquad \text{trans pathway} \qquad (R3.2)$$

$$BrO + CH_3Br \rightarrow HOBr + CH_2Br \qquad \text{cis pathway} \qquad (R4.1)$$

$$BrO + CH_3Br \rightarrow HOBr + CH_2Br \qquad \text{trans pathway} \qquad (R4.2)$$

The aim of this study is to provide rate constant expressions for these reactions. This is particularly important in view of the lack of experimental data for these reactions. In this work, highly-correlated ab initio quantum chemical calculations were

dx.doi.org/10.1021/jp301557c | J. Phys. Chem. A 2012, 116, 4396−4408

performed in order to directly compute the vibrationally adiabatic barriers for the title reactions without any further adjustments of these barriers. The energetics of these reactions was used together with TST calculations to compute the rate constants over the temperature range of 300−2500 K. To our knowledge, it is the first time that the barriers for these reactions are computed with a highly-correlated ab initio molecular orbital theory without recurring to empirical fitting schemes or indirect methods.

This article is organized as follows. Computational methods are reported in section 2, while the results are presented and discussed in section 3.

2. COMPUTATIONAL METHODS

Theoretical calculations were performed using the Gaussian03[22] software package. Reactants, transition states (TSs), pre- and post-reactive molecular complexes (MCR and MCP, respectively), and products were fully optimized with the B3LYP[23,24] and MP2[25] methods using the cc-pVTZ Dunning's correlation consistent basis set.[26−30] All TSs were characterized by one imaginary frequency (first-order saddle point) on the potential energy surface (PES). Special care was taken to determine minimum energy pathways (MEPs), performing intrinsic reaction coordinate analyses (IRC)[31,32] at all levels of theory, in order to confirm that a specific TS connects the different local minima. Vibrational frequencies and zero-point vibrational energies (ZPEs) were determined within the harmonic approximation, at the same level of theory as that used for geometries. The calculated vibrational frequencies were multiplied by an appropriate scaling factor[33] (0.965 and 0.950 for the B3LYP/cc-pVTZ and MP2/cc-pVTZ levels of theory, respectively). For all stationary points (reactants, TSs, molecular complexes, and products), single-point energy calculations (SPCs) were carried out at different high levels of theory using, in each case, the optimized B3LYP and MP2 geometrical parameters. Electronic energies were obtained by employing the single and double coupled cluster theory with inclusion of a perturbative estimation for triple excitation (CCSD(T))[34−38] using the cc-pVTZ and cc-pVQZ basis sets on geometries previously optimized with the Dunning-type cc-pVTZ basis set. The frozen-core approximation has been applied in CCSD(T) calculations, which implies that the inner shells are excluded when estimating the correlation energy.

Spin−orbit coupling is of importance, especially in the case of halogen atoms.[8,39−41] The electronic energy of the chlorine atom Cl ($^2P_{3/2}$) was obtained by subtracting one-third of the $^2P_{3/2}$−$^2P_{1/2}$ experimental splitting of the chlorine atom (−3.51 kJ mol^{-1})[42] from the calculated electronic energy of the chlorine atom Cl ($^2P_{3/2}$). Spin−orbit corrections[43] of 1.92 and −5.79 kJ mol^{-1} were added to the potential energies of ClO and BrO radicals, respectively. The potential energies of the pre-reactive molecular complexes incorporated the spin−orbit corrections of the reactants. The value was −3.51 kJ mol^{-1} for MCR_{ref}. The value for the $MCR_{1.1}$, $MCR_{1.2}$, $MCR_{2.1}$, and $MCR_{2.2}$ was −1.92 kJ mol^{-1}. In the case of the reaction of BrO with CH_3X (X = Cl, Br), the value for $MCR_{3.1}$, $MCR_{3.2}$, $MCR_{4.1}$, and $MCR_{4.2}$ was −5.79 kJ mol^{-1}. In the TSs, the spin−orbit interaction is assumed to be negligible due to the spin delocalization. Similar results have been obtained for TS structures involving iodine-containing species.[8,41,44,45]

Canonical TST[46−53] was used to predict the temperature dependence of the rate constants. Accordingly, the high-pressure limit rate constants, $k(T)$, were computed using the following expression:

$$k(T) = \Gamma(T) \times \frac{k_B T}{h} \times \frac{Q_{TS}(T)}{\prod Q_{reactants}(T)} \times \exp\left(-\frac{E_0}{k_B T}\right) \quad \text{(II-1)}$$

where $\Gamma(T)$ indicates the transmission coefficient used for the tunneling correction at temperature T and the terms $Q_{TS}(T)$ and $Q_{reactants}(T)$ are the total partition functions for the TS and the reactants at the temperature T. In eq II-1, the vibrationally adiabatic barrier height, E_0, is computed as the energy difference between the TS and the reactants, including ZPE corrections. k_B is Boltzman's constant and h is Planck's constant.

The calculation of reaction rate constants using the TST formulation given by eq II-1 requires the computation of partition functions for the reactants and the TSs. The total partition function $Q(T)$ of a species can be cast in terms of the translational $Q_{trans}(T)$, electronic $Q_{elec}(T)$, rotational $Q_{rot}(T)$, and vibrational $Q_{vib}(T)$ partition functions according to eq II-2:

$$Q(T) = Q_{trans}(T)Q_{elec}(T)Q_{rot}(T)Q_{vib}(T) \quad \text{(II-2)}$$

The partition functions were calculated using the rigid rotor harmonic oscillator model. $\Gamma(T)$ is calculated as the ratio of the quantum mechanical to the classical barrier crossing rate, assuming an unsymmetrical one-dimensional Eckart function barrier.[54] This method approximates the potential by a one-dimensional function that is fitted to reproduce the ZPE-corrected barrier, the enthalpy of reaction at 0 K, and the curvature of the potential curve at the TS. The numerical integration program of Brown[55] has been applied to obtain the $\Gamma(T)$ values at each level of theory. The rate constant calculations were performed over the temperature range of interest using the KISTHEP software.[56]

3. RESULTS AND DISCUSSION

3.1. Geometric Parameters and Vibrational Frequencies. Figures 1−9 show the potential energy profiles, the structures, and atom numbering of the TSs and molecular complexes for the nine studied pathways at the CCSD(T)/cc-pVQZ//MP2/cc-pVTZ level of theory. Tables 2−6 list the structural parameters for all TSs, pre-reactive (MCR) and post-

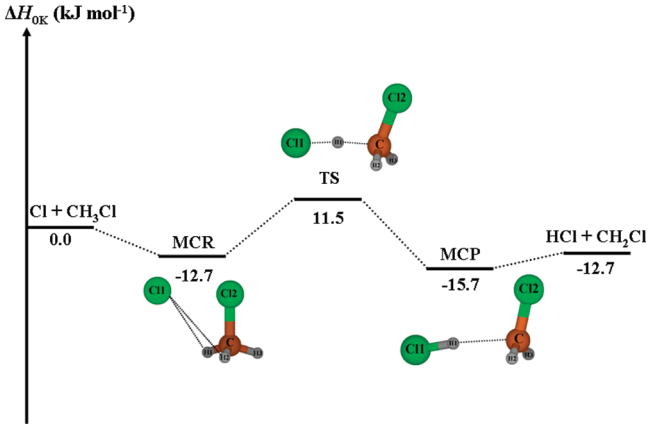

Figure 1. Potential energy profile for the reaction Cl ($^2P_{3/2}$) + CH_3Cl → HCl + CH_2Cl (R_{ref}) calculated at the CCSD(T)/cc-pVQZ//MP2/cc-pVTZ level of theory.

dx.doi.org/10.1021/jp301557c | J. Phys. Chem. A 2012, 116, 4396−4408

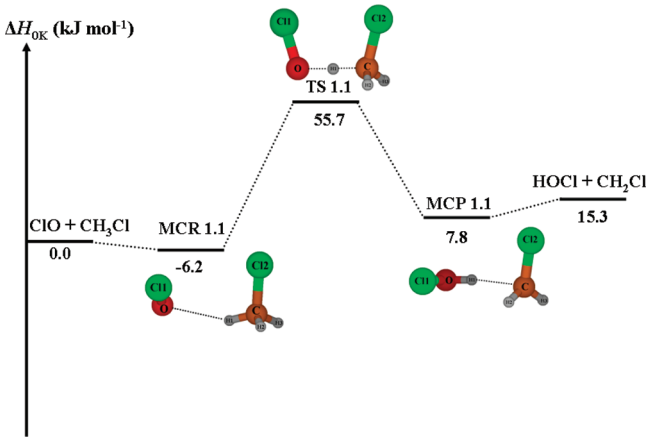

Figure 2. Potential energy profile for the cis pathway of the reaction ClO + CH_3Cl → HOCl + CH_2Cl ($R_{1.1}$) calculated at the CCSD(T)/cc-pVQZ//MP2/cc-pVTZ level of theory.

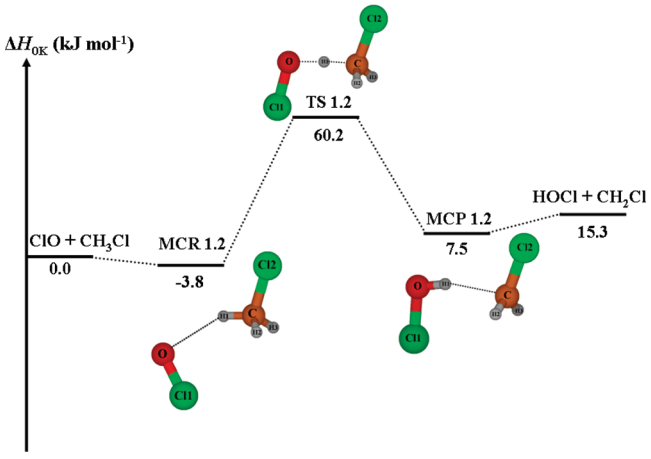

Figure 3. Potential energy profile for the trans pathway of the reaction ClO + CH_3Cl → HOCl + CH_2Cl ($R_{1.2}$) calculated at the CCSD(T)/cc-pVQZ//MP2/cc-pVTZ level of theory.

reactive (MCP) molecular complexes, and the unscaled imaginary vibrational frequencies for all TSs at the B3LYP/cc-pVTZ and MP2/cc-pVTZ levels of theory. More detailed

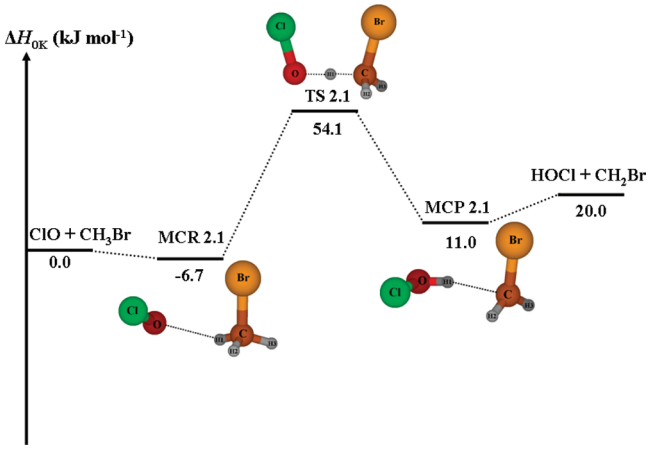

Figure 4. Potential energy profile for the cis pathway of the reaction ClO + CH_3Br → HOCl + CH_2Br ($R_{2.1}$) calculated at the CCSD(T)/cc-pVQZ//MP2/cc-pVTZ level of theory.

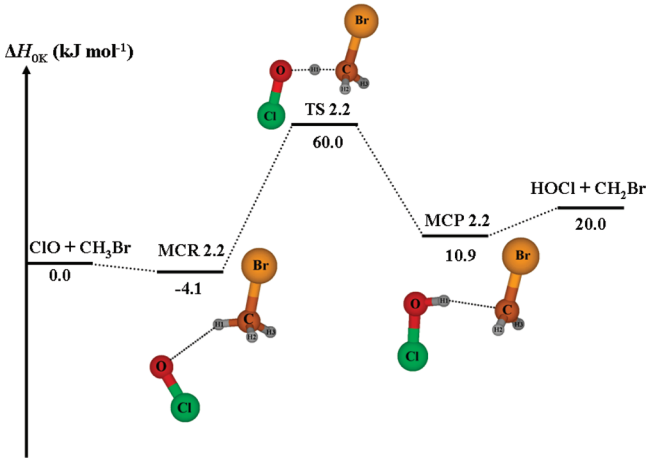

Figure 5. Potential energy profile for the trans pathway of the reaction ClO + CH_3Br → HOCl + CH_2Br ($R_{2.2}$) calculated at the CCSD(T)/cc-pVQZ//MP2/cc-pVTZ level of theory.

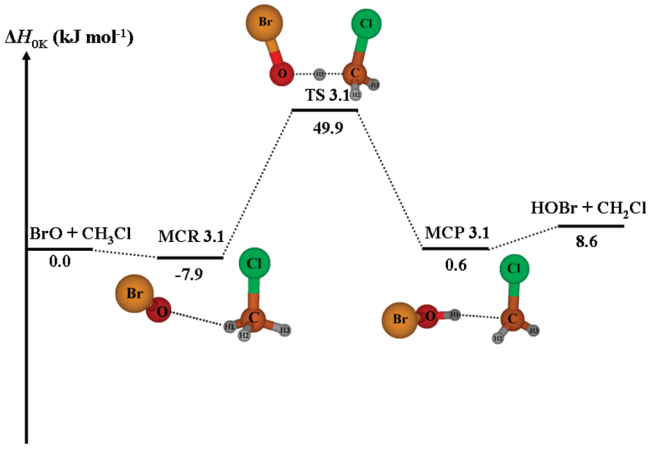

Figure 6. Potential energy profile for the cis pathway of the reaction BrO + CH_3Cl → HOBr + CH_2Cl ($R_{3.1}$) calculated at the CCSD(T)/cc-pVQZ//MP2/cc-pVTZ level of theory.

information regarding the optimized Cartesian coordinates for reactants, MCRs, MCPs, TSs, and products are given in Tables

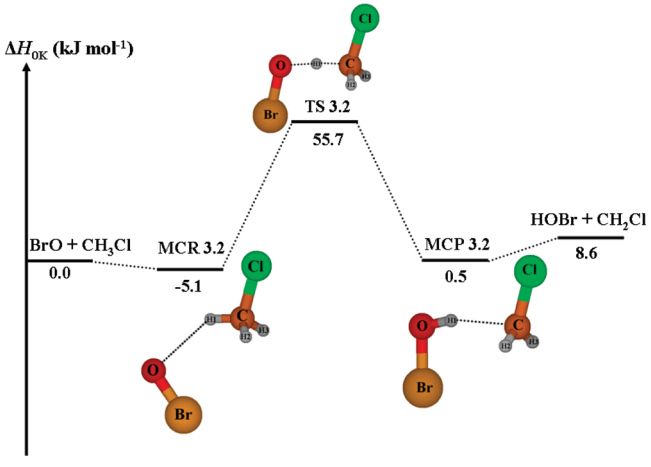

Figure 7. Potential energy profile for the trans pathway of the reaction BrO + CH_3Cl → HOBr + CH_2Cl ($R_{3.2}$) calculated at the CCSD(T)/cc-pVQZ//MP2/cc-pVTZ level of theory.

dx.doi.org/10.1021/jp301557c | J. Phys. Chem. A 2012, 116, 4396−4408

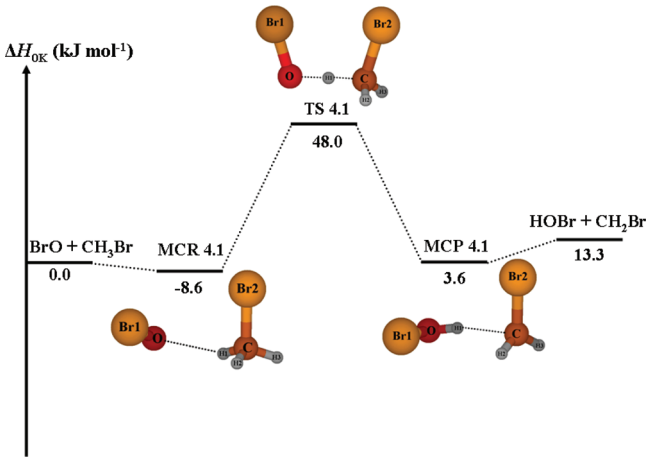

Figure 8. Potential energy profile for the cis pathway of the reaction BrO + CH_3Br → HOBr + CH_2Br ($R_{4.1}$) calculated at the CCSD(T)/cc-pVQZ//MP2/cc-pVTZ level of theory.

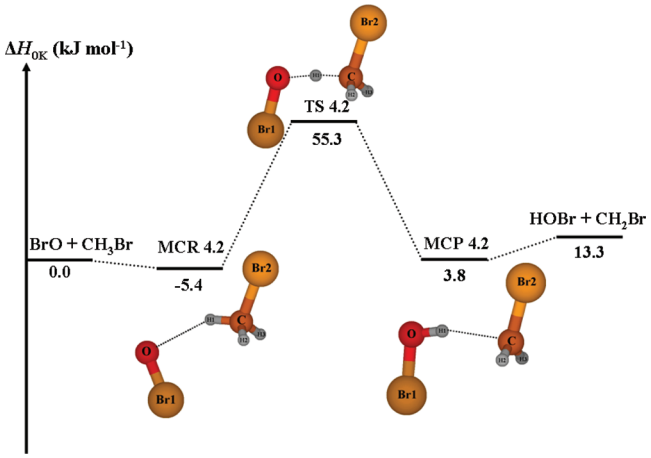

Figure 9. Potential energy profile for the trans pathway of the reaction BrO + CH_3Br → HOBr + CH_2Br ($R_{4.2}$) calculated at the CCSD(T)/cc-pVQZ//MP2/cc-pVTZ level of theory.

1S−13S of the Supporting Information. Structural parameters for the reactants and the products at the B3LYP/cc-pVTZ and MP2/cc-pVTZ levels of theory are gathered in Tables 14S and 15S of the Supporting Information, while calculated unscaled vibrational frequencies for each stationary point are reported in Table 16S of the Supporting Information.

Geometric Parameters for Transition States. The TS structure of the H-abstraction for the reaction Cl ($^2P_{3/2}$) + CH_3Cl → HCl + CH_2Cl (R_{ref}) shows that Cl1, H1, C, and Cl2 atoms are in the same plane. The dihedral angle ϕ(Cl1−H1−C−Cl2) has been estimated to be 180° at the B3LYP/cc-pVTZ and MP2/cc-pVTZ levels of theory. The unpaired electron on the Cl ($^2P_{3/2}$) atom attacks the H1−C σ-bond of the CH_3Cl molecule, and the two electrons of the σ-bond become unpaired.

In the case of the reactions involving the XO radicals (X = Cl, Br), cis and trans mechanisms have been identified on the PES for reactions R_1−R_4. The TS structures of the H-abstraction from CH_3Cl and CH_3Br by the ClO and BrO radicals show that the atoms participating in the reaction coordinate are nearly in the same plane. The dihedral angles ϕ(X−O−C−X) (X = Cl, Br) have been estimated to be nearly 0° for the cis pathway and 180° for the trans pathway at the B3LYP/cc-pVTZ and MP2/cc-pVTZ levels of theory. For reactions R_1−R_4, the unpaired electron on the XO radicals (X = Cl, Br) attacks the H1−C σ-bond of the CH_3X molecules (X = Cl, Br), and the two electrons of the σ-bond become unpaired. The main change in the geometrical structure of the TS can be characterized by the *L* parameter, defined as the ratio of the increase in the length of the bond being broken over the increase in the length of the bond being formed.[21] This parameter provides a reliable measure of the reactant- or product-like character of the TS. An *L* value larger than 1 corresponds to a product-like TS, while an *L* value smaller than 1 corresponds to a reactant-like TS. The values of the *L* parameter for each studied reaction are given in the Tables 2−6. For the reaction R_{ref}, the *L* value was estimated to be 2.1 and 0.8 at the B3LYP/cc-pVTZ and MP2/cc-pVTZ levels of theory, respectively. For the eight cis and trans pathways, *L*

Table 2. Structural Parameters[a] and Unscaled Imaginary Frequencies for the TSs and Molecular Complexes of the Reaction Cl ($^2P_{3/2}$) + CH_3Cl → HCl + CH_2Cl (R_{ref}) at B3LYP/cc-pVTZ and MP2/cc-pVTZ Levels of Theory

	B3LYP/cc-pVTZ			MP2/cc-pVTZ		
	MCR_{ref}	TS_{ref}	MCP_{ref}	MCR_{ref}	TS_{ref}	MCP_{ref}
r(Cl1−H1)	3.350	1.451	1.298	3.314	1.512	1.281
r(H1−C)	1.083	1.437	2.231	1.083	1.278	2.282
r(C−Cl2)	1.804	1.721	1.705	1.782	1.721	1.694
r(C−H2)	1.083	1.082	1.078	1.083	1.083	1.075
r(C−H3)	1.085	1.082	1.078	1.083	1.083	1.075
θ(Cl1−H1−C)	83.4	174.4	173.2	85.4	174.1	174.6
θ(H1−C−Cl2)	107.6	108.1	106.4	108.2	107.4	97.3
θ(H1−C−H2)	111.3	100.3	92.0	110.5	102.8	95.6
θ(H1−C−H3)	111.5	100.3	92.0	110.9	102.8	95.7
ϕ(Cl1−H1−C−Cl2)	−45.4	−180.0	−179.8	−49.1	180.0	−179.7
ϕ(Cl1−H1−C−H2)	72.2	−60.6	−61.2	69.2	−60.4	−61.4
ϕ(Cl1−H1−C−H3)	−162.5	60.6	61.6	−167.5	60.4	62.1
$\nu^{\ddagger}$, cm^{-1}		843i			1150i	
L^b		2.1			0.8	

[a]Bond lengths *r* are in angstroms, bond angles θ and dihedral angles ϕ are in degrees. [b]The parameter *L* is defined as the ratio of the increase in the length of the bond being broken over the increase in the length of the bond being formed, each with respect to its equilibrium value in the reactant and the product.

dx.doi.org/10.1021/jp301557c | J. Phys. Chem. A 2012, 116, 4396−4408

Table 3. Structural Parameters[a] and Unscaled Imaginary Frequencies for the TSs and Molecular Complexes of the cis and trans[b] Pathways for the Reaction ClO + CH_3Cl → HOCl + CH_2Cl ($R_{1.1}$ and $R_{1.2}$) at B3LYP/cc-pVTZ and MP2/cc-pVTZ Levels of Theory

	B3LYP/cc-pVTZ			MP2/cc-pVTZ		
	$MCR_{1.1}$ ($MCR_{1.2}$)	$TS_{1.1}$ ($TS_{1.2}$)	$MCP_{1.1}$ ($MCP_{1.2}$)	$MCR_{1.1}$ ($MCR_{1.2}$)	$TS_{1.1}$ ($TS_{1.2}$)	$MCP_{1.1}$ ($MCP_{1.2}$)
r(Cl1−O)	1.592 (1.593)	1.670 (1.673)	1.708 (1.707)	1.567 (1.570)	1.647 (1.634)	1.695 (1.695)
r(O−H1)	2.574 (2.622)	1.186 (1.197)	0.975 (0.976)	2.496 (2.563)	1.280 (1.285)	0.973 (0.973)
r(H1−C)	1.085 (1.085)	1.344 (1.325)	2.200 (2.190)	1.083 (1.083)	1.220 (1.209)	2.205 (2.187)
r(C−Cl2)	1.804 (1.802)	1.738 (1.739)	1.705 (1.705)	1.781 (1.780)	1.738 (1.741)	1.694 (1.694)
r(C−H2)	1.085 (1.085)	1.084 (1.084)	1.078 (1.078)	1.084 (1.084)	1.088 (1.084)	1.076 (1.076)
r(C−H3)	1.085 (1.085)	1.084 (1.084)	1.078 (1.078)	1.083 (1.084)	1.088 (1.084)	1.075 (1.076)
θ(Cl1−O−H1)	104.9 (111.7)	107.3 (108.1)	103.2 (102.8)	96.3 (94.5)	108.7 (107.3)	101.5 (101.4)
θ(O−H1−C)	168.4 (168.7)	177.4 (178.4)	166.1 (171.7)	149.0 (150.6)	178.9 (174.7)	165.5 (164.6)
θ(H1−C−Cl2)	108.2 (108.4)	107.1 (107.6)	107.0 (106.3)	108.4 (108.8)	108.1 (107.6)	95.4 (102.2)
θ(H1−C−H2)	110.9 (110.8)	104.0 (103.7)	92.0 (92.2)	110.6 (110.4)	105.1 (105.5)	88.4 (93.6)
θ(H1−C−H3)	110.9 (110.8)	103.8 (103.7)	91.7 (92.2)	110.7 (110.4)	105.1 (105.5)	104.6 (93.6)
ϕ(Cl1−O−H1−C)	24.4 (−2.3)	176.4 (0.0)	160.8 (0.0)	−32.7 (−0.3)	0.0 (0.0)	25.8 (0.0)
ϕ(Cl1−O−C−Cl2)	16.8 (179.8)	−5.5 (180.0)	−28.7 (180.0)	−60.9 (178.7)	0.0 (180.0)	−86.7 (−180.0)
ϕ(O−H1−C−Cl2)	−7.4 (−178.0)	178.2 (−180.0)	171.8 (−180.0)	−30.1 (179.2)	0.0 (180.0)	−112.4 (−180.0)
ϕ(O−H1−C−H2)	110.9 (−59.6)	−62.8 (−60.8)	−69.5 (−61.4)	88.6 (−61.8)	119.7 (−60.5)	4.5 (−61.3)
ϕ(O−H1−C−H3)	−125.8 (63.6)	59.2 (60.8)	53.2 (61.4)	−148.8 (60.3)	−119.6 (60.5)	127.8 (61.3)
$\nu^{\ddagger}$, cm^{-1}		1651i (1662i)			2309i (2382i)	
L^c		1.2 (1.0)			0.4 (0.4)	

[a]Bond lengths r are in angstroms, bond angles θ and dihedral angles ϕ are in degrees. [b]The values for the trans pathway (reaction $R_{1.2}$) are presented in parentheses. [c]The parameter L is defined as the ratio of the increase in the length of the bond being broken over the increase in the length of the bond being formed, each with respect to its equilibrium value in the reactant and the product.

Table 4. Structural Parameters[a] and Unscaled Imaginary Frequencies for the TSs and Molecular Complexes of the cis and trans[b] Pathways for the Reaction ClO + CH_3Br → HOCl + CH_2Br ($R_{2.1}$ and $R_{2.2}$) at B3LYP/cc-pVTZ and MP2/cc-pVTZ Levels of Theory

	B3LYP/cc-pVTZ			MP2/cc-pVTZ		
	$MCR_{2.1}$ ($MCR_{2.2}$)	$TS_{2.1}$ ($TS_{2.2}$)	$MCP_{2.1}$ ($MCP_{2.2}$)	$MCR_{2.1}$ ($MCR_{2.2}$)	$TS_{2.1}$ ($TS_{2.2}$)	$MCP_{2.1}$ ($MCP_{2.2}$)
r(Cl−O)	1.592 (1.593)	1.670 (1.674)	1.709 (1.707)	1.567 (1.570)	1.624 (1.633)	1.695 (1.695)
r(O−H1)	2.560 (2.610)	1.177 (1.187)	0.976 (0.976)	2.481 (2.544)	1.275 (1.279)	0.973 (0.973)
r(H1−C)	1.083 (1.084)	1.355 (1.334)	2.167 (2.173)	1.083 (1.082)	1.223 (1.211)	2.200 (2.176)
r(C−Br)	1.962 (1.960)	1.891 (1.893)	1.859 (1.860)	1.927 (1.926)	1.882 (1.887)	1.837 (1.837)
r(C−H2)	1.083 (1.084)	1.083 (1.083)	1.078 (1.078)	1.083 (1.083)	1.083 (1.083)	1.076 (1.076)
r(C−H3)	1.083 (1.084)	1.083 (1.083)	1.078 (1.078)	1.083 (1.083)	1.083 (1.083)	1.075 (1.076)
θ(Cl−O−H1)	109.1 (110.9)	107.0 (108.4)	103.0 (102.9)	96.3 (95.0)	106.4 (107.7)	101.4 (101.4)
θ(O−H1−C)	172.6 (168.1)	176.2 (178.3)	170.3 (172.4)	149.7 (150.7)	179.4 (175.0)	164.5 (165.6)
θ(H1−C−Br)	107.6 (107.8)	106.8 (107.1)	104.7 (105.5)	107.9 (108.3)	106.5 (106.8)	93.6 (98.3)
θ(H1−C−H2)	111.5 (111.4)	104.4 (104.1)	93.9 (93.2)	111.0 (110.8)	106.1 (105.9)	88.6 (95.2)
θ(H1−C−H3)	111.5 (111.4)	104.4 (104.4)	32.7 (93.2)	111.1 (110.8)	106.1 (105.9)	105.9 (95.2)
ϕ(Cl−O−H1−C)	10.3 (0.0)	179.5 (19.1)	98.0 (19.8)	−30.0 (−1.3)	0.1 (0.0)	28.6 (0.0)
ϕ(Cl−O−C−Br)	15.9 (180.0)	−0.5 (−173.6)	−120.8 (−173.0)	−65.1 (178.1)	0.0 (−180.0)	−87.7 (180.0)
ϕ(O−H1−C−Br)	5.8 (−180.0)	−179.9 (167.5)	143.3 (167.6)	−37.4 (179.5)	−0.1 (180.0)	116.0 (180.0)
ϕ(O−H1−C−H2)	−111.7 (−62.3)	−61.3 (−73.8)	−97.9 (−73.7)	80.8 (−62.1)	118.8 (−60.8)	−124.5 (−61.5)
ϕ(O−H1−C−H3)	123.4 (62.3)	61.4 (48.6)	24.9 (48.9)	−155.6 (61.1)	−119.0 (60.8)	−1.1 (61.5)
$\nu^{\ddagger}$, cm^{-1}		1623i (1651i)			2300i (2402i)	
L^c		1.3 (1.1)			0.5 (0.4)	

[a]Bond lengths r are in angstroms, bond angles θ and dihedral angles ϕ are in degrees. [b]The values for the trans pathway (reaction $R_{2.2}$) are presented in parentheses. [c]The parameter L is defined as the ratio of the increase in the length of the bond being broken over the increase in the length of the bond being formed, each with respect to its equilibrium value in the reactant and the product.

values were calculated to be nearly 1 at the B3LYP/cc-pVTZ level of theory and smaller than 1 at the MP2/cc-pVTZ level of theory. It is worth noticing that the L parameter does not depend on the reaction involving ClO and BrO radicals but rather on the method B3LYP or MP2. The MP2 method predicts a relatively "early" TS on the PES, where the breaking C−H bond is stretched by only a small amount from its equilibrium value in CH_3X. In addition, we notice that the MP2 method predicts shorter C−H bonds and longer O−H bonds than the corresponding B3LYP values.

Geometric Parameters for Molecular Complexes. The IRC calculations at the B3LYP/cc-pVTZ and MP2/cc-pVTZ levels of theory have revealed that the MEPs connect the TSs to loosely bound dipole−dipole complexes in both the forward

dx.doi.org/10.1021/jp301557c | J. Phys. Chem. A 2012, 116, 4396−4408

Table 5. Structural Parameters[a] and Unscaled Imaginary Frequencies for the TSs and Molecular Complexes of the cis and trans[b] Pathways for the Reaction BrO + CH_3Cl → HOBr + CH_2Cl ($R_{3.1}$ and $R_{3.2}$) at B3LYP/cc-pVTZ and MP2/cc-pVTZ Levels of Theory

	B3LYP/cc-pVTZ			MP2/cc-pVTZ		
	$MCR_{3.1}$ ($MCR_{3.2}$)	$TS_{3.1}$ ($TS_{3.2}$)	$MCP_{3.1}$ ($MCP_{3.2}$)	$MCR_{3.1}$ ($MCR_{3.2}$)	$TS_{3.1}$ ($TS_{3.2}$)	$MCP_{3.1}$ ($MCP_{3.2}$)
r(Br−O)	1.730 (1.731)	1.803 (1.807)	1.842 (1.841)	1.703 (1.706)	1.749 (1.758)	1.822 (1.822)
r(O−H1)	2.511 (2.607)	1.192 (1.204)	0.974 (0.974)	2.474 (2.582)	1.291 (1.299)	0.973 (0.973)
r(H1−C)	1.085 (1.085)	1.334 (1.316)	2.220 (2.218)	1.083 (1.083)	1.214 (1.202)	2.212 (2.197)
r(C−Cl)	1.805 (1.802)	1.740 (1.741)	1.705 (1.705)	1.781 (1.780)	1.740 (1.743)	1.694 (1.694)
r(C−H2)	1.085 (1.085)	1.084 (1.084)	1.078 (1.078)	1.084 (1.084)	1.083 (1.084)	1.075 (1.076)
r(C−H3)	1.085 (1.085)	1.084 (1.084)	1.078 (1.078)	1.084 (1.084)	1.083 (1.084)	1.076 (1.076)
θ(Br−O−H1)	112.4 (111.0)	108.4 (109.5)	103.6 (103.3)	97.9 (96.4)	107.3 (107.9)	101.6 (101.5)
θ(O−H1−C)	175.2 (168.0)	176.3 (178.4)	163.5 (173.0)	146.9 (141.1)	178.8 (173.7)	166.1 (164.7)
θ(H1−C−Cl)	108.2 (108.4)	107.5 (107.7)	108.0 (105.4)	108.3 (108.9)	107.3 (107.7)	94.4 (101.7)
θ(H1−C−H2)	111.0 (110.8)	103.9 (103.8)	91.1 (92.8)	110.6 (110.4)	106.0 (105.8)	89.7 (93.8)
θ(H1−C−H3)	111.0 (110.8)	104.3 (104.3)	91.1 (92.3)	110.8 (110.4)	106.0 (105.8)	104.3 (93.8)
ϕ(Br−O−H1−C)	−41.9 (0.0)	−173.2 (47.2)	152.5 (15.5)	−28.3 (−0.6)	0.0 (0.0)	−26.0 (0.0)
ϕ(Br−O−C−Cl)	−18.9 (180.0)	11.2 (−163.9)	−29.5 (−179.7)	−65.7 (179.7)	−0.1 (−180.0)	84.5 (−180.0)
ϕ(O−H1−C−Cl)	22.9 (−180.0)	−175.7 (149.3)	179.9 (165.1)	−40.1 (−179.7)	−0.1 (180.0)	110.4 (180.0)
ϕ(O−H1−C−H2)	141.2 (−61.6)	−56.8 (−91.7)	−61.5 (−76.2)	78.5 (−60.8)	119.1 (−60.5)	−6.6 (−61.4)
ϕ(O−H1−C−H3)	−95.4 (61.6)	65.2 (30.0)	61.2 (46.6)	−158.8 (61.3)	−119.3 (60.5)	−130.3 (61.4)
$\nu^{\ddagger}$, cm^{-1}		1650i (1650i)			2237i (2280i)	
L^c		1.1 (1.0)			0.4 (0.4)	

[a]Bond lengths r are in angstroms, bond angles θ and dihedral angles ϕ are in degrees. [b]The values for the trans pathway (reaction $R_{3.2}$) are presented in parentheses. [c]The parameter L is defined as the ratio of the increase in the length of the bond being broken over the increase in the length of the bond being formed, each with respect to its equilibrium value in the reactant and the product.

Table 6. Structural Parameters[a] and Unscaled Imaginary Frequencies for the TSs and Molecular Complexes of the cis and trans[b] Pathways for the Reaction BrO + CH_3Br → HOBr + CH_2Br ($R_{4.1}$ and $R_{4.2}$) at B3LYP/cc-pVTZ and MP2/cc-pVTZ Levels of Theory

	B3LYP/cc-pVTZ			MP2/cc-pVTZ		
	$MCR_{4.1}$ ($MCR_{4.2}$)	$TS_{4.1}$ ($TS_{4.2}$)	$MCP_{4.1}$ ($MCP_{4.2}$)	$MCR_{4.1}$ ($MCR_{4.2}$)	$TS_{4.1}$ ($TS_{4.2}$)	$MCP_{4.1}$ ($MCP_{4.2}$)
r(Br1−O)	1.730 (1.731)	1.803 (1.807)	1.841 (1.841)	1.703 (1.706)	1.746 (1.757)	1.822 (1.823)
r(O−H1)	2.488 (2.596)	1.182 (1.194)	0.974 (0.975)	2.458 (2.513)	1.288 (1.292)	0.973 (0.973)
r(H1−C)	1.084 (1.084)	1.347 (1.325)	2.204 (2.201)	1.083 (1.082)	1.215 (1.203)	2.210 (2.187)
r(C−Br2)	1.963 (1.961)	1.894 (1.895)	1.859 (1.860)	1.928 (1.927)	1.885 (1.889)	1.837 (1.838)
r(C−H2)	1.083 (1.084)	1.083 (1.083)	1.078 (1.078)	1.083 (1.083)	1.083 (1.084)	1.076 (1.076)
r(C−H3)	1.084 (1.084)	1.083 (1.083)	1.078 (1.078)	1.083 (1.083)	1.083 (1.084)	1.075 (1.076)
θ(Br1−O−H1)	114.3 (109.7)	108.2 (109.7)	103.7 (103.3)	97.8 (95.8)	107.2 (108.4)	101.6 (101.5)
θ(O−H1−C)	170.3 (165.1)	175.3 (178.2)	165.8 (172.8)	147.2 (149.5)	179.6 (173.8)	164.7 (165.5)
θ(H1−C−Br2)	107.5 (107.9)	107.2 (107.2)	107.2 (105.7)	107.9 (108.4)	106.9 (107.0)	92.5 (96.8)
θ(H1−C−H2)	111.5 (111.4)	104.4 (104.3)	92.5 (93.4)	111.0 (110.8)	106.4 (106.2)	89.8 (95.9)
θ(H1−C−H3)	111.7 (111.4)	104.8 (104.8)	92.0 (92.6)	111.2 (110.8)	106.4 (106.2)	105.6 (95.9)
ϕ(Br1−O−H1−C)	80.2 (0.0)	−172.8 (44.9)	158.3 (14.2)	−28.5 (0.2)	−179.5 (0.0)	−30.6 (0.0)
ϕ(Br1−O−C−Br2)	42.7 (180.0)	9.6 (−166.5)	−34.5 (−179.7)	−69.8 (179.4)	0.0 (180.0)	86.2 (−180.0)
ϕ(O−H1−C−Br2)	−37.2 (−180.0)	−177.8 (149.0)	168.8 (166.5)	−44.2 (179.3)	179.5 (180.0)	116.4 (−180.0)
ϕ(O−H1−C−H2)	−154.7 (−62.3)	−59.1 (−92.3)	−72.4 (−74.7)	73.9 (−62.3)	−61.5 (−60.8)	−0.7 (−61.6)
ϕ(O−H1−C−H3)	80.2 (62.3)	63.5 (30.1)	50.2 (48.0)	−162.5 (60.9)	60.6 (60.8)	124.5 (61.6)
$\nu^{\ddagger}$, cm^{-1}		1626i (1644i)			2230i (2305i)	
L^c		1.2 (1.1)			0.4 (0.4)	

[a]Bond lengths r are in angstroms, bond angles θ and dihedral angles ϕ are in degrees. [b]The values for the trans pathway (reaction $R_{4.2}$) are presented in parentheses. [c]The parameter L is defined as the ratio of the increase in the length of the bond being broken over the increase in the length of the bond being formed, each with respect to its equilibrium value in the reactant and the product.

and backward directions. For the reaction R_{ref}, the Cl1, H1, C, and Cl2 atoms in the pre-reactive molecular complex structure (MCR_{ref}) are not in the same plane. The Cl1 atom forms two intermolecular bonds with two hydrogens of chloromethane, while in the post-reactive molecular complex (MCP_{ref}), the dihedral angle ϕ(Cl1−H1−C−Cl2) has been estimated to be 180° at B3LYP/cc-pVTZ and MP2/cc-pVTZ levels of theory. The dihedral angles ϕ(X−O−C−X) (X = Cl, Br) in the MCR complexes have been calculated for the cis pathways $R_{1.1}$, $R_{2.1}$, $R_{3.1}$, and $R_{4.1}$. The corresponding values are 16.8, 15.9, 18.9, and 42.7° at the B3LYP/cc-pVTZ level of theory and 60.9, 65.1, 65.7, and 69.8° at the MP2/cc-pVTZ level of theory. The dihedral angles ϕ(X−O−C−X) (X = Cl, Br) for the cis pathways $R_{1.1}$, $R_{2.1}$, $R_{3.1}$, and $R_{4.1}$ have been estimated in the

dx.doi.org/10.1021/jp301557c | J. Phys. Chem. A 2012, 116, 4396−4408

Table 7. Reaction Enthalpies $\Delta_r H$ at 0 K and Standard Reaction Enthalpies[a] $\Delta_r H°$ at 298 K (in kJ mol^{-1}) Calculated at Different Levels of Theory Including Spin−Orbit Corrections for the Different Studied Reactions

SPC level of theory	Cl ($^2P_{3/2}$) + CH_3Cl → HCl + CH_2Cl (R_{ref})	ClO + CH_3Cl → HOCl + CH_2Cl ($R_{1.1-2}$)	ClO + CH_3Br → HOCl + CH_2Br ($R_{2.1-2}$)	BrO + CH_3Cl → HOBr + CH_2Cl ($R_{3.1-2}$)	BrO + CH_3Br → HOBr + CH_2Br ($R_{4.1-2}$)
CCSD(T)/cc-pVTZ//B3LYP/cc-pVTZ	−8.6 (−4.8)	14.6 (16.7)	18.2 (20.4)	9.9 (12.6)	13.5 (16.3)
CCSD(T)/cc-pVQZ//B3LYP/cc-pVTZ	−14.1 (−10.3)	14.3 (16.4)	18.5 (20.7)	7.9 (10.5)	12.0 (14.8)
CCSD(T)/cc-pVTZ//MP2/cc-pVTZ	−7.2 (−3.8)	14.9 (16.5)	18.9 (20.5)	10.3 (12.5)	14.3 (16.5)
CCSD(T)/cc-pVQZ//MP2/cc-pVTZ	−12.7 (−9.2)	15.3 (16.9)	20.0 (21.6)	8.6 (10.8)	13.3 (15.5)
experimental value (literature) at 298 K	(−14.4 ± 3.8)	(22.8 ± 5.0)	(30.3 ± 6.8)	(12.5 ± 6.5)	(20.0 ± 8.3)

[a]The standard reaction enthalpies at 298 K are presented in parentheses.

MCP complexes. Their values are 28.7, 120.8, 29.5, and 34.5° at the B3LYP/cc-pVTZ level of theory and 86.7, 87.7, 84.5, and 86.2° at the MP2/cc-pVTZ level of theory. For the trans pathways $R_{1.2}$, $R_{2.2}$, $R_{3.2}$, and $R_{4.2}$, the dihedral angles ϕ(X−O−C−X) (X = Cl, Br) for the pre- and post-reactive molecular complexes have been calculated to be close to 180° at both levels of theory.

Reaction R_{ref}. The TS is connected to the Cl···CH_3Cl reactant complex (MCR_{ref}) and also to the ClH···CH_2Cl product complex (MCP_{ref}). When the chlorine atom approaches the CH_3Cl molecule, it forms two intermolecular bonds Cl1···H1 and Cl1···H2 of 3.350 and 3.314 Å at the B3LYP/cc-pVTZ and MP2/cc-pVTZ levels of theory, respectively. On the product side, the structure of MCP_{ref} has been determined with an intermolecular bond H1···C of 2.231 and 2.282 Å at the B3LYP/cc-pVTZ and MP2/cc-pVTZ levels of theory, respectively.

Reaction R_1. The $TS_{1.1}$ (cis) and the $TS_{1.2}$ (trans) are connected to the ClO···CH_3Cl reactant complexes $MCR_{1.1}$ and $MCR_{1.2}$, respectively, and also to the ClOH···CH_2Cl product complexes $MCP_{1.1}$ and $MCP_{1.2}$, respectively. When the ClO radical approaches the CH_3Cl molecule on the cis pathway, it forms an intermolecular bond O···H1 of 2.574 and 2.496 Å for the cis pathway at the B3LYP/cc-pVTZ and MP2/cc-pVTZ levels of theory, respectively (2.622 and 2.563 Å for the trans pathway, respectively). On the product side, the structures of $MCP_{1.1}$ and $MCP_{1.2}$ have been determined with an intermolecular bond H1···C of 2.200 and 2.205 Å for the cis pathway at the B3LYP/cc-pVTZ and MP2/cc-pVTZ levels of theory, respectively (2.190 and 2.187 Å for the trans pathway, respectively).

Reaction R_2. The $TS_{2.1}$ (cis) and $TS_{2.2}$ (trans) are connected to the ClO···CH_3Br reactant complexes $MCR_{2.1}$ and $MCR_{2.2}$, respectively, and also to the ClOH···CH_2Br product complexes $MCP_{2.1}$ and $MCP_{2.2}$, respectively. When the ClO radical approaches the CH_3Br molecule on the cis pathway, it forms an intermolecular bond O···H1 of 2.560 and 2.481 Å for the cis pathway at the B3LYP/cc-pVTZ and MP2/cc-pVTZ levels of theory, respectively (2.610 and 2.544 Å for the trans pathway, respectively). On the product side, the structures of $MCP_{2.1}$ and $MCP_{2.2}$ have been determined with an intermolecular bond H1···C of 2.167 and 2.200 Å for the cis pathway at the B3LYP/cc-pVTZ and MP2/cc-pVTZ levels of theory, respectively (2.173 and 2.176 Å for the trans pathway, respectively).

Reaction R_3. The $TS_{3.1}$ (cis) and $TS_{3.2}$ (trans) are connected to the BrO···CH_3Cl reactant complexes $MCR_{3.1}$ and $MCR_{3.2}$, respectively, and also to the BrOH···CH_2Cl product complexes $MCP_{3.1}$ and $MCP_{3.2}$, respectively. When the BrO radical approaches the CH_3Cl molecule on the cis pathway, it forms an intermolecular bond O···H1 of 2.511 and 2.474 Å at the B3LYP/cc-pVTZ and MP2/cc-pVTZ levels of theory, respectively (2.607 and 2.582 Å for the trans pathway, respectively). On the product side, the structures of $MCP_{3.1}$ and $MCP_{3.2}$ have been determined with an intermolecular bond H1···C of 2.220 and 2.212 Å for the cis pathway at the B3LYP/cc-pVTZ and MP2/cc-pVTZ levels of theory, respectively (2.218 and 2.197 for the trans pathway, respectively).

Reaction R_4. The $TS_{4.1}$ (cis) and $TS_{4.2}$ (trans) are connected to the BrO···CH_3Br reactant complexes $MCR_{4.1}$ and $MCR_{4.2}$, respectively, and also to the BrOH···CH_2Br product complexes $MCP_{4.1}$ and $MCP_{4.2}$, respectively. When the BrO radical approaches the CH_3Br molecule on the cis pathway, it forms an intermolecular bond O···H1 of 2.488 and 2.458 Å at the B3LYP/cc-pVTZ and MP2/cc-pVTZ levels of theory, respectively (2.596 and 2.513 Å for the trans pathway, respectively). On the product side, the structures of $MCP_{4.1}$ and $MCP_{4.2}$ have been determined with an intermolecular bond H1···C of 2.204 and 2.210 Å for the cis pathway at the B3LYP/cc-pVTZ and MP2/cc-pVTZ levels of theory, respectively (2.201 and 2.187 Å for the trans pathway, respectively).

Vibrational Frequencies. In all cases, the eigenvector in the TS corresponding to the imaginary frequency is primarily a motion of the atom being transferred. The imaginary frequencies at the MP2/cc-pVTZ level of theory are larger than those obtained at the B3LYP/cc-pVTZ level of theory.

3.2. Energetics. Table 7 lists for the nine studied reactions the calculated reaction enthalpy at 0 K $\Delta_r H$(0 K) and the standard reaction enthalpy at 298 K $\Delta_r H°$(298 K), including spin−orbit corrections at the CCSD(T)/cc-pVnZ//B3LYP/cc-pVTZ and CCSD(T)/cc-pVnZ//MP2/cc-pVTZ levels of theory (n = T, Q). At both levels of theory, the reaction of Cl ($^2P_{3/2}$) atoms with CH_3Cl is exothermic, while the reactions of the XO radical with CH_3X (X = Cl, Br) are endothermic. As can be observed in Table 7, the computed reaction enthalpies at 0 and 298 K depend slightly on the geometry optimization level of theory. The basis set employed with the CCSD(T) single-point energy calculation does affect slightly the $\Delta_r H$(0 K) and $\Delta_r H°$(298 K) values, especially for the reaction R_{ref}. Increasing the basis set size in the single-point calculation from cc-pVTZ to cc-pVQZ changes the value of $\Delta_r H$(0 K) by about −6 kJ mol^{-1} for the reaction R_{ref}, while the changes for the reactions R_1−R_4 range from −2.0 to +1.1 kJ mol^{-1}. The $\Delta_r H°$(298 K) values have been also calculated using the literature standard enthalpies of formation at 298 K for the species of interest[9] (see Table 17S of the Supporting Information). The corresponding literature values are also listed for each reaction in Table 7. The

dx.doi.org/10.1021/jp301557c | J. Phys. Chem. A 2012, 116, 4396−4408

Table 8. Vibrationally Adiabatic Barriers E_0 Calculated (in kJ mol^{-1}) for cis and trans[a] Pathways at Different Levels of Theory Including Spin−Orbit Corrections

SPC level of theory	Cl ($^2P_{3/2}$) + CH_3Cl → HCl + CH_2Cl (R_{ref})	ClO + CH_3Cl → HOCl + CH_2Cl ($R_{1.1-2}$)	ClO + CH_3Br → HOCl + CH_2Br ($R_{2.1-2}$)	BrO + CH_3Cl → HOBr + CH_2Cl ($R_{3.1-2}$)	BrO + CH_3Br → HOBr + CH_2Br ($R_{4.1-2}$)
CCSD(T)/cc-pVTZ//B3LYP/cc-pVTZ	14.5	56.0 (59.4)	54.8 (59.0)	52.6 (56.6)	51.1 (56.0)
CCSD(T)/cc-pVQZ//B3LYP/cc-pVTZ	8.1	55.6 (59.5)	54.1 (59.0)	50.7 (55.4)	48.9 (54.7)
CCSD(T)/cc-pVTZ//MP2/cc-pVTZ	17.2	55.4 (58.9)	54.4 (58.8)	51.3 (55.9)	49.9 (55.5)
CCSD(T)/cc-pVQZ//MP2/cc-pVTZ	11.5	55.7 (60.2)	54.1 (60.0)	49.9 (55.7)	48.0 (55.3)

[a]The vibrationally adiabatic barriers for the trans pathways are presented in parentheses.

Table 9. Relative Enthalpies at 0 K (in kJ mol^{-1}) for the Pre-reactive (MCR) and Post-reactive[a] (MCP) Complexes for cis and trans[b] Pathways at Different Levels of Theory Including Spin−Orbit Corrections

	Cl ($^2P_{3/2}$) + CH_3Cl → HCl + CH_2Cl (R_{ref})	
SPC level of theory	MCR_{ref}	MCP_{ref}
CCSD(T)/cc-pVTZ//B3LYP/cc-pVTZ	−11.4	−9.3/*−0.7*
CCSD(T)/cc-pVQZ//B3LYP/cc-pVTZ	−16.5	−15.2/*−1.1*
CCSD(T)/cc-pVTZ//MP2/cc-pVTZ	−8.8	−9.9/*−2.7*
CCSD(T)/cc-pVQZ//MP2/cc-pVTZ	−12.7	−15.7/*−3.0*
	ClO + CH_3Cl → HOCl + CH_2Cl ($R_{1.1}$ and $R_{1.2}$)	
	$MCR_{1.1}$ ($MCR_{1.2}$)	$MCP_{1.1}$ ($MCP_{1.2}$)
CCSD(T)/cc-pVTZ//B3LYP/cc-pVTZ	−2.6 (−4.2)	9.2 (8.3)/*−5.4 (−6.3)*
CCSD(T)/cc-pVQZ//B3LYP/cc-pVTZ	−1.7 (−3.2)	9.1 (8.1)/*−5.2 (−6.2)*
CCSD(T)/cc-pVTZ//MP2/cc-pVTZ	−6.5 (−4.6)	7.5 (7.1)/*−7.4 (−7.8)*
CCSD(T)/cc-pVQZ//MP2/cc-pVTZ	−6.2 (−3.8)	7.8 (7.5)/*−7.5 (−7.8)*
	ClO + CH_3Br → HOCl + CH_2Br ($R_{2.1}$ and $R_{2.2}$)	
	$MCR_{2.1}$ ($MCR_{2.2}$)	$MCP_{2.1}$ ($MCP_{2.2}$)
CCSD(T)/cc-pVTZ//B3LYP/cc-pVTZ	−6.5 (−4.5)	11.6 (11.2)/*−6.6 (−7.0)*
CCSD(T)/cc-pVQZ//B3LYP/cc-pVTZ	−5.6 (−3.5)	11.9 (11.4)/*−6.6 (−7.1)*
CCSD(T)/cc-pVTZ//MP2/cc-pVTZ	−6.9 (−4.9)	10.3 (10.2)/*−8.6 (−8.7)*
CCSD(T)/cc-pVQZ//MP2/cc-pVTZ	−6.7 (−4.1)	11.0 (10.9)/*−9.0 (−9.1)*
	BrO + CH_3Cl → HOBr + CH_2Cl ($R_{3.1}$ and $R_{3.2}$)	
	$MCR_{3.1}$ ($MCR_{3.2}$)	$MCP_{3.1}$ ($MCP_{3.2}$)
CCSD(T)/cc-pVTZ//B3LYP/cc-pVTZ	−7.1 (−5.3)	4.2 (3.5)/*−5.7 (−6.4)*
CCSD(T)/cc-pVQZ//B3LYP/cc-pVTZ	−6.1 (−4.1)	2.2 (1.5)/*−5.7 (−6.4)*
CCSD(T)/cc-pVTZ//MP2/cc-pVTZ	−8.1 (−5.8)	2.5 (2.2)/*−7.8 (−8.1)*
CCSD(T)/cc-pVQZ//MP2/cc-pVTZ	−7.9 (−5.1)	0.6 (0.5)/*−8.0 (−8.1)*
	BrO + CH_3Br → HOBr + CH_2Br ($R_{4.1}$ and $R_{4.2}$)	
	$MCR_{4.1}$ ($MCR_{4.2}$)	$MCP_{4.1}$ ($MCP_{4.2}$)
CCSD(T)/cc-pVTZ//B3LYP/cc-pVTZ	−7.5 (−5.6)	7.0 (6.3)/*−6.5 (−7.2)*
CCSD(T)/cc-pVQZ//B3LYP/cc-pVTZ	−6.6 (−4.5)	5.3 (4.8)/*−6.7 (−7.2)*
CCSD(T)/cc-pVTZ//MP2/cc-pVTZ	−8.6 (−6.2)	5.2 (5.2)/*−9.1 (−9.1)*
CCSD(T)/cc-pVQZ//MP2/cc-pVTZ	−8.6 (−5.4)	3.6 (3.8)/*−9.7 (−9.5)*

[a]Values in italic correspond to the relative enthalpies at 0 K in kJ mol^{-1} with respect to the products. [b]The relative enthalpies at 0 K for the trans pathway are presented in parentheses.

calculated $\Delta_r H°(298\ K)$ are in fair agreement with their literature counterparts if the experimental uncertainties are taken into consideration.

Table 8 shows for the reactions R_{ref} and R_1−R_4 the computed vibrationally adiabatic barriers E_0 including the literature spin−orbit corrections at the four different levels of theory. The reaction R_{ref} has a relatively small electronic barrier by comparison to those of reactions of XO radicals with CH_3X (X = Cl, Br). The vibrationally adiabatic barrier E_0 for the reaction R_{ref} is sensitive to the basis set employed in the CCSD(T) single-point energy calculation. Increasing the basis set size from cc-pVTZ to cc-pVQZ decreases the E_0 values of R_{ref} by about 6−7 kJ mol^{-1}. Reactions R_1−R_4 have large E_0 values ranging from 48.0 to 56.0 kJ mol^{-1} for the cis pathways and from 54.7 to 60.2 kJ mol^{-1} for the trans pathways at the CCSD(T)/cc-pVnZ//B3LYP/cc-pVTZ and CCSD(T)/cc-pVTnZ//MP2/cc-pVTZ (n = T, Q) levels of theory. For the four reactions R_1−R_4, E_0 depends slightly on the basis set size employed in the CCSD(T) single-point calculation.

Table 9 lists the relative enthalpies at 0 K for the pre- and post-reactive complexes at different levels of theory. The MCR complexes are more stable than the reactants at each level of theory. The stabilization enthalpies at 0 K range from 1.7 to 8.6 kJ mol^{-1} and 3.2 to 6.2 kJ mol^{-1} for the cis and trans pathways,

dx.doi.org/10.1021/jp301557c | J. Phys. Chem. A 2012, 116, 4396−4408

Table 10. Calculated Rate Constants[a] at Different Temperatures (in cm^3 $molecule^{-1}$ s^{-1}) at Different Levels of Theory for the Reaction Cl ($^2P_{3/2}$) + CH_3Cl → HCl + CH_2Cl (R_{ref})

	temperature (K)					
SPC level of theory	300	600	1000	1500	2000	2500
CCSD(T)/cc-pVTZ//B3LYP/cc-pVTZ	8.08×10^{-14}	2.38×10^{-12}	1.87×10^{-11}	7.68×10^{-11}	1.87×10^{-10}	3.52×10^{-10}
CCSD(T)/cc-pVQZ//B3LYP/cc-pVTZ	9.85×10^{-13}	8.56×10^{-12}	4.05×10^{-11}	1.29×10^{-10}	2.76×10^{-10}	4.80×10^{-10}
CCSD(T)/cc-pVTZ//MP2/cc-pVTZ	4.68×10^{-14}	1.67×10^{-12}	1.47×10^{-11}	6.44×10^{-11}	1.62×10^{-10}	3.10×10^{-10}
CCSD(T)/cc-pVQZ//MP2/cc-pVTZ	4.19×10^{-13}	5.20×10^{-12}	2.93×10^{-11}	1.02×10^{-10}	2.29×10^{-10}	4.09×10^{-10}

[a]Values obtained with the Kisthep software.

respectively. The MCP complexes are more stable than the products at each level of theory. The stabilization enthalpies at 0 K range from 5.4 to 9.7 kJ mol^{-1} and 6.2 to 9.5 kJ mol^{-1} for the cis and trans pathways, respectively. Increasing the basis set size has little effect on the $\Delta_r H(0\ K)$ of MCR and MCP complexes.

3.3. Kinetic Parameters Calculations. *Rate Constants.* The calculations of the temperature dependence of rate constants have been performed at four different levels of theory for the reaction of Cl ($^2P_{3/2}$) atoms with CH_3Cl and the reactions of XO radicals with CH_3X (X = Cl, Br).

Cl ($^2P_{3/2}$) + CH_3Cl → HCl + CH_2Cl R_{ref}. Table 10 lists the rate constants calculated at fours levels of theory for six different temperatures (300, 600, 1000, 1500, 2000, and 2500 K). Literature values derived from experiments with different setups,[12−19] data evaluations,[9−11] and those estimated by theoretical approaches[20,21] (based on structure−activity relationships and BAC-MP4 calculations both combined with TST) are given in Table 1. As presented in Table 10, the computed rate constants at 300 K range from 4.68×10^{-14} to 9.85×10^{-13} cm^3 $molecule^{-1}$ s^{-1}, showing the strong dependence of the rate constant on the level of theory. The values of the rate constants calculated at 300 K at the CCSD(T)/cc-pVTZ//B3LYP/cc-pVTZ, CCSD(T)/cc-pVQZ//B3LYP/cc-pVTZ, CCSD(T)/cc-pVTZ//MP2/cc-pVTZ, and CCSD(T)/cc-pVQZ//MP2/cc-pVTZ levels of theory are 8.08×10^{-14}, 9.85×10^{-13}, 4.68×10^{-14}, and 4.19×10^{-13} cm^3 $molecule^{-1}$ s^{-1}, respectively. The rate constants calculated at 300 K using the CCSD(T)/cc-pVQZ//MP2/cc-pVTZ level of theory are in good agreement with the different experimental determinations and the last compilation made by Sander et al.[9] (4.9×10^{-13} cm^3 $molecule^{-1}$ s^{-1}). The rate constant estimated at 300 K at the CCSD(T)/cc-pVQZ//B3LYP/cc-pVTZ level of theory is higher by about a factor of 2 than the one estimated at the CCSD(T)/cc-pVQZ//MP2/cc-pVTZ level of theory. The values of the rate constants calculated at 300 K at the CCSD(T)/cc-pVTZ//B3LYP/cc-pVTZ and CCSD(T)/cc-pVTZ//MP2/cc-pVTZ levels of theory are smaller by about a factor of 10 than the ones obtained at the CCSD(T)/cc-pVQZ//B3LYP/cc-pVTZ and CCSD(T)/cc-pQTZ//MP2/cc-pVTZ levels of theory. The differences between the calculated rate constants and their literature counterparts (calculated from the Arrhenius expression; see Table 1) are however less and less marked as the temperature rises. For example, we observe at 600 K a good agreement between the experimental values of 3.82×10^{-12} and 1.08×10^{-11} cm^3 $molecule^{-1}$ s^{-1} (by Bryukov et al.[12] and Clyne and Walker,[16] respectively) and our calculated values at the CCSD(T)/cc-pVnZ//B3LYP/cc-pVTZ and CCSD(T)/cc-pVnZ//MP2/cc-pVTZ (n = T, Q) levels of theory (2.38×10^{-12}, 8.56×10^{-12}, 1.67×10^{-12}, and 5.20×10^{-12} cm^3 $molecule^{-1}$ s^{-1}, respectively). By comparison to the experimental values obtained by Bryukov et al.[12] at 300 and 600 K, the most appropriate level of theory to compute quantitatively the temperature dependence of the rate constant is the CCSD(T)/cc-pVQZ//MP2/cc-pVTZ level of theory, which shows the closest ratios k_{calc}/k_{exp} (0.78 and 1.36 at 300 and 600 K, respectively).

XO + CH_3X → HOX + CH_2X (X = Cl, Br) (R_1−R_4). For the reactions involving ClO and BrO radicals, it can be observed that the calculated rate constants at 300 K do depend markedly on the geometry optimization level of theory. For example, for the reaction of the ClO radical with CH_3Cl, the rate constants at 300 K are 3.37×10^{-21}, 3.93×10^{-21}, 1.81×10^{-20}, and 1.62×10^{-20} cm^3 $molecule^{-1}$ mol^{-1} at the CCSD(T)/cc-pVTZ//B3LYP/cc-pVTZ, CCSD(T)/cc-pVQZ//B3LYP/cc-pVTZ, CCSD(T)/cc-pVTZ//MP2/cc-pVTZ, and CCSD(T)/cc-pVQZ//MP2/cc-pVTZ levels of theory, respectively. A fair agreement is observed between the literature value of 8.07×10^{-21} cm^3 $molecule^{-1}$ s^{-1} estimated by Ho et al.[5] (value derived from their two-parameter Arrhenius expression) and our calculations. At higher temperatures (T > 1000 K), the calculated rate constants for the reaction R_1 are greater by about 1−2 orders of magnitude than the ones estimated by Ho et al.[5] The influence of the basis set size on the calculated rate constants for all reactions is however less and less marked as the temperature rises (see Tables 18S−25S of the Supporting Information). It is worth noticing that the nature of the halogen atom in the XO radical or in the CH_3X molecule does not have a marked impact on the calculated rate constant. Concerning the cis or trans nature of the pathway, the rate constant of the trans pathway is always higher than that of the corresponding cis pathway by a factor varying from 1.1 to 3.6 over the temperature range of 650−2500 K.

As CH_3Cl reacts with other radicals than ClO in combustion mechanisms, it is interesting to compare the rate constant of reaction ClO + CH_3Cl → HOCl + CH_2Cl ($R_{1.2}$) with those of H-abstraction reactions from CH_3Cl by other radicals to determine if reaction $R_{1.2}$ can be competitive. In the combustion mechanism of chloromethane developed by Wang et al.,[57] H-abstraction reactions from CH_3Cl by H, OH, O, HO_2, and CH_3 radicals are also included in addition to reaction $R_{1.2}$. At 1000 K, the rate constant of the reaction ClO + CH_3Cl → HOCl + CH_2Cl ($R_{1.2}$) calculated at the CCSD(T)/cc-pVQZ//MP2/cc-pVTZ level of theory is lower by a factor of 119, 52, and 36 than that of H-abstraction reaction by H, OH, and O radicals, respectively. However, it is higher by a factor 65 and 4 than that of reactions with less reactive HO_2 and CH_3 radicals, respectively. As the temperature increases, the rate constant of reaction $R_{1.2}$ becomes comparable to that of H-abstraction reactions by H, OH, and O radicals. For example, at 2000 K, the rate constant of reaction $R_{1.2}$ is only lower by a factor of 5 than that of the H-abstraction

dx.doi.org/10.1021/jp301557c | J. Phys. Chem. A 2012, 116, 4396−4408

Table 11. Summary of the Arrhenius Parameters Calculated over the Temperature Range of 300−2500 K for the Studied Reactions

reaction		SPC level of theory	A_1[a]	n_1	$E_{a,1}$[b]	A_2[a]	n_2	$E_{a,2}$[b]
$Cl\ (^2P_{3/2}) + CH_3Cl \rightarrow HCl + CH_2Cl$	(Rref)	CCSD(T)/cc-pVTZ//B3LYP/cc-pVTZ	2.30×10^{-12}	2.14	8.40	1.37×10^{-11}	1.81	22.80
		CCSD(T)/cc-pVQZ//B3LYP/cc-pVTZ	2.70×10^{-12}	2.12	2.56	1.49×10^{-11}	1.76	17.44
		CCSD(T)/cc-pVTZ//MP2/cc-pVTZ	1.45×10^{-12}	2.17	8.68	1.04×10^{-11}	1.92	21.59
		CCSD(T)/cc-pVQZ//MP2/cc-pVTZ	1.93×10^{-12}	2.14	3.88	1.19×10^{-11}	1.85	17.54
$ClO + CH_3Cl \rightarrow HOCl + CH_2Cl$ cis pathway	(R1.1)	CCSD(T)/cc-pVTZ//B3LYP/cc-pVTZ	1.35×10^{-13}	3.20	49.97	1.11×10^{-15}	3.91	31.94
		CCSD(T)/cc-pVQZ//B3LYP/cc-pVTZ	1.35×10^{-13}	3.20	49.59	1.12×10^{-15}	3.91	31.57
		CCSD(T)/cc-pVTZ//MP2/cc-pVTZ	2.40×10^{-14}	3.38	42.69	1.06×10^{-16}	3.86	21.79
		CCSD(T)/cc-pVQZ//MP2/cc-pVTZ	1.21×10^{-16}	3.80	22.40	2.47×10^{-14}	3.37	43.05
$ClO + CH_3Cl \rightarrow HOCl + CH_2Cl$ trans pathway	(R1.2)	CCSD(T)/cc-pVTZ//B3LYP/cc-pVTZ	1.03×10^{-15}	4.03	34.28	1.87×10^{-13}	3.19	53.56
		CCSD(T)/cc-pVQZ//B3LYP/cc-pVTZ	9.91×10^{-16}	4.04	34.26	1.88×10^{-13}	3.19	53.67
		CCSD(T)/cc-pVTZ//MP2/cc-pVTZ	8.37×10^{-14}	3.43	45.90	1.34×10^{-16}	4.47	21.72
		CCSD(T)/cc-pVQZ//MP2/cc-pVTZ	7.96×10^{-14}	3.45	46.88	1.19×10^{-16}	4.46	22.49
$ClO + CH_3Br \rightarrow HOCl + CH_2Br$ cis pathway	(R2.1)	CCSD(T)/cc-pVTZ//B3LYP/cc-pVTZ	1.16×10^{-13}	3.19	49.00	1.69×10^{-15}	3.74	32.80
		CCSD(T)/cc-pVQZ//B3LYP/cc-pVTZ	1.16×10^{-13}	3.19	48.36	1.83×10^{-15}	3.72	32.39
		CCSD(T)/cc-pVTZ//MP2/cc-pVTZ	1.26×10^{-16}	4.28	22.67	2.76×10^{-14}	3.24	43.80
		CCSD(T)/cc-pVQZ//MP2/cc-pVTZ	3.04×10^{-14}	3.19	44.18	1.34×10^{-16}	4.41	22.81
$ClO + CH_3Br \rightarrow HOCl + CH_2Br$ trans pathway	(R2.2)	CCSD(T)/cc-pVTZ//B3LYP/cc-pVTZ	1.65×10^{-15}	3.90	35.37	1.93×10^{-13}	3.21	53.21
		CCSD(T)/cc-pVQZ//B3LYP/cc-pVTZ	1.92×10^{-13}	3.21	53.25	1.65×10^{-15}	3.90	35.41
		CCSD(T)/cc-pVTZ//MP2/cc-pVTZ	9.28×10^{-14}	3.38	46.74	2.72×10^{-16}	4.29	24.20
		CCSD(T)/cc-pVQZ//MP2/cc-pVTZ	9.07×10^{-14}	3.39	47.78	2.63×10^{-16}	4.27	25.23
$BrO + CH_3Cl \rightarrow HOBr + CH_2Cl$ cis pathway	(R3.1)	CCSD(T)/cc-pVTZ//B3LYP/cc-pVTZ	1.01×10^{-15}	3.93	28.73	1.28×10^{-13}	3.19	46.99
		CCSD(T)/cc-pVQZ//B3LYP/cc-pVTZ	1.06×10^{-15}	3.92	26.96	1.30×10^{-13}	3.19	45.19
		CCSD(T)/cc-pVTZ//MP2/cc-pVTZ	2.38×10^{-14}	3.37	39.17	1.04×10^{-16}	3.87	18.62
		CCSD(T)/cc-pVQZ//MP2/cc-pVTZ	1.18×10^{-16}	3.72	17.55	2.33×10^{-14}	3.38	37.61
$BrO + CH_3Cl \rightarrow HOBr + CH_2Cl$ trans pathway	(R3.2)	CCSD(T)/cc-pVTZ//B3LYP/cc-pVTZ	1.19×10^{-13}	3.18	51.24	6.08×10^{-16}	4.03	31.67
		CCSD(T)/cc-pVQZ//B3LYP/cc-pVTZ	1.22×10^{-13}	3.17	50.07	6.01×10^{-16}	4.03	30.37
		CCSD(T)/cc-pVTZ//MP2/cc-pVTZ	2.41×10^{-16}	3.67	21.35	6.75×10^{-14}	3.47	42.69
		CCSD(T)/cc-pVQZ//MP2/cc-pVTZ	6.24×10^{-14}	3.50	42.12	2.43×10^{-16}	3.50	20.99
$BrO + CH_3Br \rightarrow HOBr + CH_2Br$ cis pathway	(R4.1)	CCSD(T)/cc-pVTZ//B3LYP/cc-pVTZ	9.21×10^{-14}	3.20	45.59	1.29×10^{-15}	3.77	29.10
		CCSD(T)/cc-pVQZ//B3LYP/cc-pVTZ	9.48×10^{-14}	3.20	43.29	1.43×10^{-15}	3.74	27.14
		CCSD(T)/cc-pVTZ//MP2/cc-pVTZ	1.35×10^{-16}	4.05	19.35	2.25×10^{-14}	3.32	38.84
		CCSD(T)/cc-pVQZ//MP2/cc-pVTZ	1.48×10^{-16}	4.17	17.79	2.54×10^{-14}	3.26	37.63
$BrO + CH_3Br \rightarrow HOBr + CH_2Br$ trans pathway	(R4.2)	CCSD(T)/cc-pVTZ//B3LYP/cc-pVTZ	7.22×10^{-16}	3.95	32.27	9.60×10^{-14}	3.20	50.61
		CCSD(T)/cc-pVQZ//B3LYP/cc-pVTZ	7.56×10^{-16}	3.92	31.08	9.61×10^{-14}	3.20	49.29
		CCSD(T)/cc-pVTZ//MP2/cc-pVTZ	8.06×10^{-14}	3.40	43.53	2.52×10^{-16}	4.09	21.75
		CCSD(T)/cc-pVQZ//MP2/cc-pVTZ	7.90×10^{-14}	3.41	43.19	2.48×10^{-16}	4.06	21.43

[a]Unit: cm^3 $molecule^{-1}$ s^{-1}. [b]Unit: kJ mol^{-1}.

reaction by the H atom and is almost equal to that of H-abstraction reactions by OH and O radicals.

Arrhenius Parameters. The calculated rate constants $k(T)$ at the four levels of theory can be best fit by a double exponential (due to a marked curvature) over the temperature range of 300−2500 K according to eq III-1

$$k(T) = A_1\left(\frac{T}{300}\right)^{n_1}\exp\left(-\frac{E_{a,1}}{RT}\right) + A_2\left(\frac{T}{300}\right)^{n_2}\exp\left(-\frac{E_{a,2}}{RT}\right) \quad \text{(III-1)}$$

The values of the parameters A_1, n_1, $E_{a,1}$, A_2, n_2, and $E_{a,2}$ are listed in Table 11. The first step of this work concerning the rate constant estimation of the reaction $Cl\ (^2P_{3/2}) + CH_3Cl \rightarrow HCl + CH_2Cl$ has shown that the CCSD(T)/cc-pVQZ//MP2/

dx.doi.org/10.1021/jp301557c | J. Phys. Chem. A 2012, 116, 4396−4408

Table 12. Summary of the Arrhenius Parameters Calculated at the CCSD(T)/cc-pVQZ//MP2/cc-pVTZ Level of Theory over the Temperature Range of 600−2500 K for the Studied Reactions

reaction		A^a	n	$E_a{}^b$
$ClO + CH_3Cl \rightarrow HOCl + CH_2Cl$ cis pathway	(R1.1)	6.92×10^0	3.64	9274
$ClO + CH_3Cl \rightarrow HOCl + CH_2Cl$ trans pathway	(R1.2)	1.42×10^1	3.72	10220
$ClO + CH_3Br \rightarrow HOCl + CH_2Br$ cis pathway	(R2.1)	8.46×10^0	3.59	9095
$ClO + CH_3Br \rightarrow HOCl + CH_2Br$ trans pathway	(R2.2)	1.77×10^1	3.69	10293
$BrO + CH_3Cl \rightarrow HOBr + CH_2Cl$ cis pathway	(R3.1)	7.96×10^0	3.62	8093
$BrO + CH_3Cl \rightarrow HOBr + CH_2Cl$ trans pathway	(R3.2)	1.48×10^1	3.70	9351
$BrO + CH_3Br \rightarrow HOBr + CH_2Br$ cis pathway	(R4.1)	1.04×10^1	3.57	7829
$BrO + CH_3Br \rightarrow HOBr + CH_2Br$ trans pathway	(R4.2)	2.12×10^1	3.66	9391

[a]Unit: $cm^3\ mol^{-1}\ s^{-1}$. [b]Unit: cal mol^{-1}.

cc-pVTZ level of theory is the most appropriate one to determine its rate constant quantitatively. According to this conclusion, we recommend the use of Arrhenius parameters determined at the CCSD(T)/cc-pVQZ//MP2/cc-pVTZ level of theory for the reactions R_1−R_4. For modeling combustion applications with CHEMKIN-II code,[58] the rate constants $k(T)$ estimated at the CCSD(T)/cc-pVQZ//MP2/cc-pVTZ level of theory have been fitted by a three-parameter Arrhenius expression over the temperature range of 600−2500 K. Table 12 lists the values of the three parameters for the studied reactions with the pre-exponential factor expressed in $cm^3\ mol^{-1}\ s^{-1}$ and the activation energy in cal mol^{-1}.

4. CONCLUSION

Theoretical calculations associated with canonical TST combined with an Eckart tunneling correction have been performed for the H-abstraction reactions from CH_3Cl and CH_3Br by ClO and BrO radicals. The geometrical parameters of reactants, products, pre- and post-reactive molecular complexes, and TSs have been fully optimized at the B3LYP/cc-pVTZ and MP2/cc-pVTZ levels of theory. SPCs have been performed at CCSD(T)/cc-pVTZ//B3LYP/cc-pVTZ, CCSD(T)/cc-pVQZ//B3LYP/cc-pVTZ, CCSD(T)/cc-pVTZ//MP2/cc-pVTZ, and CCSD(T)/cc-pVQZ//MP2/cc-pVTZ levels of theory. The reference reaction Cl ($^2P_{3/2}$) + $CH_3Cl \rightarrow$ HCl + CH_2Cl has been first studied to choose the appropriate level of theory for reactions involving chlorine- and bromine-containing species. The rate constants calculated using the CCSD(T)/cc-pVQZ//MP2/cc-pVTZ level of theory for the reference reaction is in good agreement with the literature counterparts. This level of theory has been used for the rate constants estimation for the reactions ClO + CH_3Cl (R_1), ClO + CH_3Br (R_2), BrO + CH_3Cl (R_3), and BrO + CH_3Br (R_4). For these four reactions, the six-parameter Arrhenius expressions have been obtained by fitting to the computed rate constants for elementary pathways over the temperature range of 300−2500 K.

■ ASSOCIATED CONTENT

Supporting Information

Additional tables as described in the text. (*i*) Optimized Cartesian coordinates for reactants, products, molecular complexes, and transition states, (*ii*) structural parameters for reactants and products, (*iii*) vibrational frequencies, (*iv*) literature enthalpies of formation at 298 K, and (*v*) estimated rate constants. This material is available free of charge via the Internet at http://pubs.acs.org.

■ AUTHOR INFORMATION

Corresponding Author

*Phone: (33)3-20434985. E-mail: sebastien.canneaux@univ-lille1.fr.

Notes

The authors declare no competing financial interest.

■ ACKNOWLEDGMENTS

We thank the ROMEO2 computational center of the University of Reims Champagne−Ardenne, the Centre de Ressources Informatiques de HAute Normandie (CRIHAN), and the Centre de Ressources Informatiques (CRI) of Lille1 Sciences and Technologies University for providing computing time for part of the theoretical calculations. The authors thank Professor Joseph W. Bozzelli (New Jersey Institute of Technology) for fruitful discussions.

■ REFERENCES

(1) Urey, H. C.; Johnston, H. *Phys. Rev.* **1931**, *38*, 2131−2152.
(2) Pannetier, G.; Gaydon, A. G. *Nature* **1948**, *161*, 242−243.
(3) Yuasa, S.; Yushina, S.; Uchida, T.; Shiraishi, N. *Proc. Combust. Inst.* **2000**, *28*, 863−870.

(4) Senkan, S. M. *Pollutants from Combustion. Formation and Impact on Atmospheric Chemistry*; NATO Sciences Series, Series C; Vovelle, C., Ed.; Kluwer Academic Press: Dordrecht, The Netherlands, 2000; p 547.
(5) Ho, W.; Yu, Q.-R.; Bozzelli, J. W. *Combust. Sci. Technol.* **1992**, *85*, 23−63.
(6) Vaidya, W. M. *Proc. Ind. Acad. Sci.* **1938**, *A7*, 321−336.
(7) Coleman, E. H.; Gaydon, A. G. *Discuss. Faraday Soc.* **1947**, *2*, 166−169.
(8) Canneaux, S.; Xerri, B.; Louis, F.; Cantrel, L. *J. Phys. Chem. A* **2010**, *114*, 9270−9288.
(9) Sander, S. P.; Friedl, R. R.; Barker, J. R.; Golden, D. M.; Kurylo, M. J.; Wine, P. H.; Abbatt, J. P. D.; Burkholder, J. B.; Kolb, C. E.; Moortgat, G. K. et al. Chemical kinetics and photochemical data for use in atmospheric studies. In *Evaluation number 17, JPL-NASA 10-6*. http://jpldataeval.jpl.nasa.gov (2011).
(10) Orlando, J. J. *Int. J. Chem. Kinet.* **1999**, *31*, 515−524.
(11) Atkinson, R.; Baulch, D. L.; Cox, R. A.; Hampson, R. F., Jr.; Kerr, J. A.; Rossi, M. J.; Troe, J. *J. Phys. Chem. Ref. Data* **1997**, *26*, 521−1011.
(12) Bryukov, M. G.; Slagle, I. R.; Knyazev, V. D. *J. Phys. Chem. A* **2002**, *106*, 10532−10542.
(13) Wallington, T. J.; Andino, J. M.; Ball, J. C.; Japar, S. M. *J. Atmos. Chem.* **1990**, *10*, 301−313.
(14) Tschuikow-Roux, E.; Yano, T.; Niedzielski, J. *J. Chem. Phys.* **1985**, *82*, 65−74.
(15) Manning, R. G.; Kurylo, M. J. *J. Phys. Chem.* **1977**, *81*, 291−296.
(16) Clyne, M. A. A.; Walker, R. F. *J. Chem. Soc., Faraday Trans. 1* **1973**, *69*, 1547−1567.
(17) Knox, J. H. *Trans. Faraday Soc.* **1962**, *58*, 275−283.
(18) Goldfinger, P.; Huybrechts, G.; Martens, G. *Trans. Faraday Soc.* **1961**, *57*, 2210−2219.
(19) Pritchard, H. O.; Pyke, J. B.; Trotman-Dickenson, A. F. *J. Am. Chem. Soc.* **1955**, *77*, 2629−2633.
(20) Senkan, S. M.; Quam, D. *J. Phys. Chem.* **1992**, *96*, 10837−10842.
(21) Rayez, M. T.; Rayez, J. C.; Sawerysyn, J. P. *J. Phys. Chem. Ref. Data* **1994**, *98*, 11342−11352.
(22) Frisch, M. J.; Trucks, G. W.; Schlegel, H. B.; Scuseria, G. E.; Robb, M. A.; Cheeseman, J. R.; Montgomery, J. A.; Vreven, T.; Kudin, K. N.; Burant, J. C. et al. *Gaussian 03*, revision D.01; Gaussian, Inc.: Wallingford, CT, 2004.
(23) Becke, A. *J. Chem. Phys.* **1993**, *98*, 5648−5652.
(24) Lee, C.; Yang, W.; Parr, R. *Phys. Rev. B* **1988**, *37*, 785−789.
(25) Møller, C.; Plesset, M. S. *Phys. Rev.* **1934**, *46*, 618.
(26) Dunning, J. T. H. *J. Chem. Phys.* **1989**, *90*, 1007−1023.
(27) Kendall, R. A.; Dunning, J. T. H.; Harrison, R. J. *J. Chem. Phys.* **1992**, *96*, 6796−6806.
(28) Woon, D. E.; Dunning, J. T. H. *J. Chem. Phys.* **1993**, *98*, 1358−1371.
(29) Peterson, K. A.; Woon, D. E.; Dunning, J. T. H. *J. Chem. Phys.* **1994**, *100*, 7410−7415.
(30) Wilson, A. K.; van Mourik, T.; Dunning, T. H. *J. Mol. Struct.: THEOCHEM* **1996**, *388*, 339−349.
(31) Gonzalez, C.; Schlegel, H. B. *J. Chem. Phys.* **1989**, *90*, 2154−2161.
(32) Gonzalez, C.; Schlegel, H. B. *J. Phys. Chem.* **1990**, *94*, 5523−5527.
(33) NIST. Computational Chemistry Comparison and Benchmark Database. Johnson, R. D., III, Ed.; *NIST Standard Reference Database Number 101*, Release 15. http://cccbdb.nist.gov/ (February 2010).
(34) Cizek, J. *Adv. Chem. Phys.* **1969**, *14*, 35−89.
(35) Purvis, G. D., III; Bartlett, R. J. *J. Chem. Phys.* **1982**, *76*, 1910−1918.
(36) Scuseria, G. E.; Janssen, C. L.; Schaefer, H. F., III. *J. Chem. Phys.* **1988**, *89*, 7382−7387.
(37) Scuseria, G. E.; Schaefer, H. F., III. *J. Chem. Phys.* **1989**, *90*, 3700−3703.
(38) Pople, J. A.; Head-Gordon, M.; Raghavachari, K. *J. Chem. Phys.* **1987**, *87*, 5968−5975.
(39) Lee, S.-H.; Liu, K. *J. Chem. Phys.* **1999**, *111*, 6253−6259.
(40) Jasper, A. W.; Klippenstein, S. J.; Harding, L. B. *J. Phys. Chem. A* **2010**, *114*, 5759−5768.
(41) Hammaecher, C.; Canneaux, S.; Louis, F.; Cantrel, L. *J. Phys. Chem. A* **2011**, *115*, 6664−6674.
(42) Moore, C. E. *Atomic Energy Levels*, NSRDS-NBS 35; USGPO: Washington, DC, 1971; Vols. *I* and *II*.
(43) Chase, M. W. *J. Phys. Chem. Ref. Data* **1998**, *Monograph 9*.
(44) Stevens, J. E.; Cui, Q.; Morokuma, K. *J. Chem. Phys.* **1998**, *108*, 1544−1551.
(45) Mečiarová, K.; Šulka, M.; Canneaux, S.; Louis, F.; Černušák, I. *Chem. Phys. Lett.* **2011**, *517*, 149−154.
(46) Eyring, H. *J. Chem. Phys.* **1935**, *3*, 107−115.
(47) Johnston, H. S. *Gas Phase Reaction Rate Theory*; The Roland Press Co.: New York, 1966.
(48) Laidler, K. J. *Theories of Chemical Reaction Rates*; McGraw-Hill: New York, 1969.
(49) Weston, R. E.; Schwartz, H. A. *Chemical Kinetics*; Prentice-Hall: New York, 1972.
(50) Rapp, D. *Statistical Mechanics*; Holt, Reinhard, and Winston: New York, 1972.
(51) Nikitin, E. E. *Theory of Elementary Atomic and Molecular Processes in Gases*; Claredon Press: Oxford, U.K., 1974.
(52) Smith, I. W. M. *Kinetics and Dynamics of Elementary Gas Reactions*; Butterworths: London, 1980.
(53) Steinfeld, J. I.; Francisco, J. S.; Hase, W. L. *Chemical Kinetics and Dynamics*; Prentice-Hall: Englewood Cliffs, NJ, 1989.
(54) Eckart, C. *Phys. Rev.* **1930**, *35*, 1303−1309.
(55) Brown, R. L. *J. Res. Natl. Bur. Stand. (U.S.)* **1981**, *86*, 357−359.
(56) Henon, E.; Bohr, F.; Canneaux, S.; Postat, B.; Auge, F.; Bouillard, E.; Domureau, V. *KISTHEP 1.0*; University of Reims Champagne-Ardenne: France, 2003.
(57) Wang, H.; Hahn, T. O.; Sung, C. J.; Law, C. K. *Combust. Flame* **1996**, *105*, 291−307.
(58) Kee, R. J.; Rupley, F. M.; Miller, J. A. *Chemkin-II: a Fortran Chemical Kinetics Code Package for the Analysis of Gas-Phase Chemical Kinetics*, SAND89-8209; Sandia National Laboratories Reports: Livermore, CA, 1989.